DETERMINATION SEVERITY OF BURN USING NEURAL NETWORK AND LANDSAT TM

K. R. AL-RAWI, J. L. CASANOVA and M. LOUAKFAOUI

kamal@latuv.uva.es

Laboratorio de Teledetección, LATUV,
Facultad de Ciencia,
Universidad de Valladolid,
47071 Valladolid

RESUMEN: Un sistema automático de cartografía de áreas quemadas usando imágenes Landsat TM ha sido desarrollado. Teniendo solo el límite de la zona del incendio, el sistema es capaz de determinar la severidad de las quemas. El mapa de la severidad de las quemas muestra la textura del área quemada, que refleja la topografía afectada y el estado de la biomasa.
La red neuronal Supervised ART-II, ha sido empleada, las bandas 3,4 y 5 han sido usadas, tanto imágenes tomadas después del incendio como imágenes multitemporal han sido incorporadas a la red.
Usando diferentes tamaños de conjuntos de aprendizaje y diferentes parámetros dinámicos se ha comprobado el rendimiento del sistema.

ABSTRACT: An automatic burned area mapping system with LandsatTM has been developed. Given only the boundary of the burned area, the system can determine the severity of burns. Burn severity map shows the texture of burned area, which reflect the affect of topography and biomass status.
The SupervisedART-II neural network has been employed. Bands 3, 4, and 5 have been used. Post-fire, as well as multi-temporal images have been incorporated in to the network.
Using different-sized training sets and different dynamic parameters have tested system performance.

Palabras clave: Teledetección, redes neuronales, incendios forestales, ART, aprendizaje supervisado.

Key words: Remote sensing, wildfires, neural network, ART, supervised learning.

INTRODUCTION

Burned area mapping by means of remote sensing data is an active field of research among scientists. Data from the National Oceanic and Atmospheric Administration (NOAA) Advanced Very High Resolution Radiometer (AVHRR), as well as the Landsat TM images are widely used in this task. Different approaches have been reported in the literature for burned area mapping using Landsat. TM. Visual inspection using false colour composites has been employed by [7] for mapping burned areas in Spain. Regression analysis has been employed by [8] for mapping burned areas in Oregon, USA. Maximum Likelihood Classifier (MLC) has employed by [10] for fire scar detection in Amazonia. Principle Component (PC) analysis and MLC have been employed by [11]. [18] Employed Kauth-Thomas and PC analysis for burned area mapping in Arizona, USA.

Artificial Neural Networks (ANN) have been employed extensively in remote sensing tasks in the last decade. However, they have not been employed for fire monitoring with the exception of the recent work by [2-4]. Burned Area Mapping System (BAMS) and Fire Detection System (FDS) has been developed in [2]. Integrated Fire Evolution Monitoring System (IFEMS), which integrate both BAMS and FDS for monitoring fire evolution, has been developed in [3]. IFEMS has the ability to differentiate among active fire, burned area, area beneath flames, and area that burned completely between two consecutive images. The IFEMS has been applied for monitoring multi-fire phenomena in Spain [4]. These articles deal with NOAA-AVHRR and oriented for monitoring fire evolution taking the advantage of relatively high temporal-resolution of the satellite. The low resolution of NOAA-AVHRR (1.1x1.1km at nadir) does not meet the user demands for mapping burned area. To our knowledge, ANNs have not been used for mapping burned areas using Landsat TM imagery, which its spatial-30x30m) meets most user demands.

OBJECTIVES

This study has been conducted to build an automatic burned area mapping system with Landsat TM images using Supervised ART-II ANN [1]. The system has the ability to determine the severity of burn at pixel level by knowing only the boundary of the burned area. Determination the burn area at pixel level of Landsat TM images by sending personal team to the field is tedious task. Determination the severity of burn is even harder.

System performance will be tested by means of different dynamic parameters. The system will be evaluated using post-fire together with multi-temporal images.

STUDY AREA

The study area is a large fire in Millares, the province of Valencia, which is located on the Mediterranean coast of eastern Spain.

DATA

Landsat TM images (a scene of 901x1181 pixels included the fire under study) correspond to June 29th, 1994 and August 19th, 1994 have been employed for the multi-temporal case. While Landsat images correspond to August 19 have been employed for post-fire case. The fire under consideration occurred July 4-13, 1994. Landsat TM, bands 3, 4, and 5 have been employed.

Ground truth data for burned areas has been adapted from the Spanish Forest Authority (ICONA). They reported only the boundary of the fire using the global positioning system. Every pixel inside the determined area was considered to be burned. Such assumption neglect the affect of topography, the condition of biomass and meteorological conditions, which influence the fire behaviour leaving some patches slightly burn or even unburned at all.

SUPERVISED ART-II ANN

The category layer of Supervised ART-II is divided into stacks. The number of stacks being equal to the number of classes. The architecture of Supervised ART-II is shown in figure 1.

Training phase

The choice function is computed for all the committed category nodes for all stacks;

$$T_{j_k k} = \frac{\sum_{i=1}^{2M} (A_i \wedge w_{ij_k k})}{\alpha + \sum_{i=1}^{2M} w_{ij_k k}}; j_k = 1...C(k); k = 1...L$$

where $w_{ij_k k}$ are the weights, which connect each category node j_k in each stack k with all input nodes i, M is the dimension of the normalized input vector A[0,1], $C(k)$ is the number of committed nodes in the stack number k, L is total number of classes, and is the choice parameter (α>0). The notation ($a \wedge w$) means $min(a, w)$ in fuzzy logic. The maximum choice value node for each stack is determined. These are the candidates of their stack to represent the current input. The winning node among these candidates is the node with the maximum choice value.

Resonance occurs if the winning node matching value is greater or equal to the predetermined vigilance parameter ρ [0,1];

$$\sum_{i=1}^{2M} (A_i \wedge w_{iJK}) / M \geq \rho$$

If both resonance and class matching are occurred the winning category node should be trained;

$$w_{iJK}^{new} = \beta(A_i \wedge w_{iJK}^{old}) + (1-\beta) w_{iJK}^{old}; i = 1...2M$$

where β [0,1] is the dynamic learning rate. Otherwise, the current stack will present its second highest choice value as its candidate. Candidates of other stacks are unchanged. Finally, either one of the committed category nodes can represent the current input (resonance and class matching occur) or a new node should be committed. In the later case, the input vector is assigned to the weight vector of the newly committed category node (fast learning mode β=1).

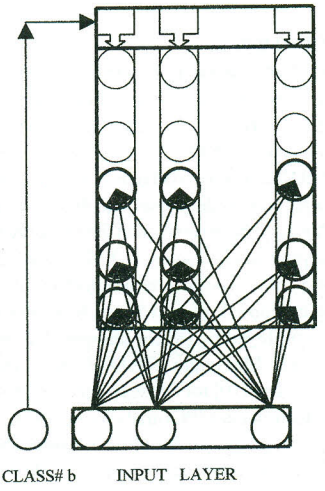

Figure 1. Architecture of Supervised ART-II.

New category node should be committed from the stack that represents the input features when all its nodes fail to represent the current input. This is because all other nodes of other stacks will not pass class matching. For more details about Supervised ART-II, please see [1].

Testing phase

The stack number K, which has the highest choice value category node, represents the class code b of the current input;

$$b = K = k \left[\max\{T_{j_k k}\}; j_k = 1..C(k); k = 1...L\right]$$

METHOD

During training phase, for each pixel, the normalized values [0,1] for band 3, band 4, band 5, and their complements are incorporated to the input layer of the neural network. At the same time the class code b of the pixel is incorporated to the memory field of the stacks to high light the correspond stack. Therefore, in the post-fire case the size of the input layer is 6 nodes, while in the multi-temporal case its size is 12 nodes. At the end of the training phase, all weights of the network are fixed. The number of category node, which each of them represents a subclass is determined.

During the testing phase the normalized values and their complements for all mentioned bands are incorporated to the network. The choice function will be computed for all category nodes. The stack number of the node that scores the highest choice value represents the class code of the current pixel.

SEVERITY OF BURN

Burn severity map is constructed through training the network with different sizes of training samples. The network has been trained with 3000, 2000, 1500, 1000, 800, 600, 500, 400, 350, 300, 250, 200, 150, 125, and 100 training samples. Number of burned pixels in all above training samples is fixed at 50 pixels. Only pixels with high severity of burns can be captured when the network is trained with large training sample. As training sample decreases pixels with less severity of burned can be mapped. The performance for mapping burned area has increased from 32.59% to 81.75% training with 3000 and 100 pixels, respectively. The grey level of the newly mapped pixels should be proportional to the training sample to highlight the severity of burn.

The burn severity map shows the textures of burned area (figure 2). Four selected areas of the burn severity map have been magnified to show clearly the detail textures of the burned area (figure 2—a, b, c & d). The burn severity map reflects the topography and the condition of biomass, while the assumed map, which depends on the boundary of the burned area, is not (figure 3). Burn scars show variation in shape and topology. They are "irregular, finger-like, have island and detached outliers (spots)" [6]. The texture of burn severity map shows these structures clearly.

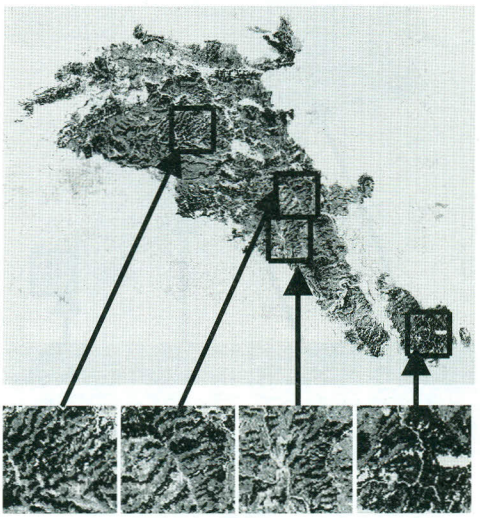

Figure 2. Constructing fire severity map using post-fire images. Fire severity map shows clearly the texture of the burned area. Selected areas have been magnified to highlight the detail texture of the burned area.

Figure 3. The assumed burned area. It has been determined by determination of the boundary of the area using Global Positioning System.

Burn severity map also has been constructed using multi-temporal images (figure 4). It does not show the texture of burned area clearly as that of post fire case (figure 2), however, the main features of the texture is in match with both severity maps.

The dynamic learning rate β=0.25 and the vigilance parameter ρ=0.98 have been employed. More details about mapping burned area and construction of severity of burn can be found in [5].

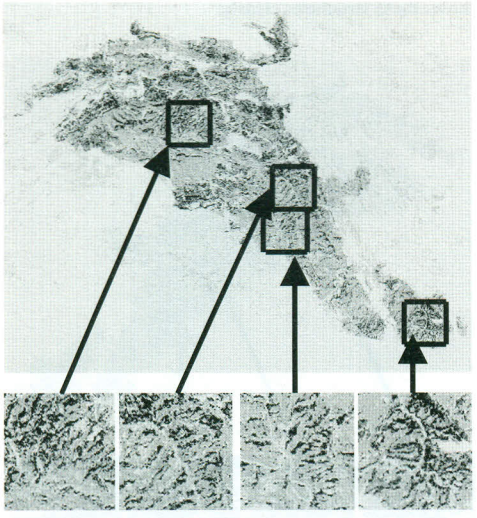

Figure 4: Constructing fire severity map using multi.-temporal images. Fire severity map using multi-temporal images is not good as post-fire images. However, it shows that the main features of burned area texture are similar to that of post fire.

CONCLUSIONS

Burn severity map can be constructed through training the network with different sizes of training samples, which conclude a fixed number of burned pixels. Only pixels with high severity of burns can be captured when the network is trained with large training sample. As training sample decreases pixels with less severity of burned can be mapped. The grey level of the newly mapped pixels should be proportional to the training sample to highlight the severity of burn.

Post-fire images are recommended for burned area mapping in simple terrain, while multi-temporal images must be employed for complex terrain in order to eliminate the effect of the topography.

REFERENCES

[1] AL-RAWI, K. R., C. GONZALO, and A. ARQUERO, "Supervised ART-II: A new neural network architecture, with quicker learning algorithm, for classifying multi-valued input patterns", *Proceeding of the European Symposium on Artificial Neural Networks ESSAN-99,* Bruges: Belgium, 289-294. 1999

[2] AL-RAWI, K. R., J. L. CASANOVA, and A. CALLE, "Burned area mapping system and fire detection system, based on neural networks and NOAA-AVHRR imagery", *International Journal of Remote Sens*ing (in press).

[3] AL-RAWI, K. R., J. L. CASANOVA, and A. ROMO, "IFEMS: New approach for monitoring wildfire evolution with NOAA-AVHRR imagery", *International Journal of Remote Sensing* (in press).

[4] AL-RAWI, K. R., J. L. CASANOVA, and E. M. LOUAKFAOUI, "IFEMS for monitoring spatial-temporal behaviour of multiple fire phenomena", *submitted to the International Journal of Remote Sensing.*

[5] AL-RAWI, K. R., J. L. CASANOVA, and A. CALLE, "ART neural network for mapping burned area and determination severity of burn with Landsat TM images" submitted to *IEEE Transaction on Geoscience and Remote Sensing.*

[6] CLARKE, K. C., J. A. BRASS, P. J. RIGGAN, "A cellular automation Model of wildfire propagation and extinction", *Photogrammetic Engineering and Remote Sensing,* 60, 1355-1367, 1994..

[7] CHUVIECO, E., R. G. CONGALTON, "Mapping and inventory of forest fires from digital processing of TM data", *Geocarto International,* 4, 41-53, 1988.

[8] KUSHLA, J. D., W. J. RIPPLE, "Assessing wildfire effects with Landsat thematic mapper data", *International Journal of Remote Sensing,* 19(13), 2493-2507, 1998.

[9] PATTERSON, M. W., S. R. YOOL, "Mapping fire-induced vegetation mortality using Landsat Thematic Mapper data: A comparision of linear transformation techniques", *Remote Sensing of Environment,* 65, 132-142, 1998.

[10] PEREIRA, M. C., A. W. SETZER, "Spectral characteristic of fire scars in Landsat-5 TM image of Amazonia", *International Journal of Remote Sensing,* 14(11), 2061-2078, 1993.

[11] SILJESTROM, P., A. MORENO, A., "Monitoring burnt areas by principle components analysis of multitemporal TM data", *Intenational Journal of Remote Sensing,* 16 (19), 1577-1587, 1995.